

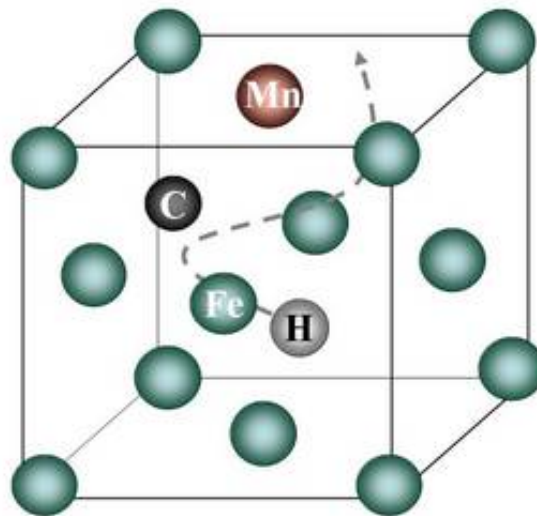
# Report

## FEM formulation for mass diffusion through UMATHT subroutine

Theory and implementation

**Author(s)**

Antonio Alvaro, Philippe Mainçon, Vidar Osen



# Report

## FEM formulation for mass diffusion through UMATHT subroutine


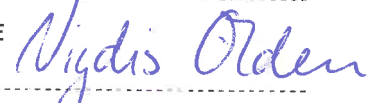
Theory and implementation

**VERSION**  
1.0**DATE**  
19th December 2014**AUTHOR(S)**

Antonio Alvaro, Philippe Mainçon, Vidar Osen

**CLIENT(S)**Research Council of Norway, Statoil,  
Technip**CLIENT'S REFERENCE****PROJECT**ROP: Knowledge basis for Repair cOntin-  
gency of Pipelines**NUMBER OF PAGES AND ATTACHMENTS**  
18**ABSTRACT**

This report summarized the development of a Finite Element framework for the description of bulk mass diffusion of a solute (hydrogen) in metallic materials (iron/steels). The implemented governing diffusion law accounts not only for the solute concentration gradients but also for the mechanical state (stress and strain) on the distribution of the solute. The different forms of the Finite Element formulations are described as well as the implementation in the Abaqus commercial code is made through the use of a user defined UMATHT subroutine. A final chapter is also dedicated to the conversion of the units for hydrogen concentration.

**PREPARED BY**  
Antonio Alvaro**SIGNATURE****CHECKED BY**  
Vigdis Olden**SIGNATURE****APPROVED BY**  
Magnus Eriksson**SIGNATURE****REPORT NUMBER**  
A26585**ISBN**  
978-82-14-05833-8**CLASSIFICATION**  
Unrestricted**CLASSIFICATION THIS PAGE**  
Unrestricted

# Document History

---

<b>VERSION</b>	<b>DATE</b>	<b>VERSION DESCRIPTION</b>
1.0	16/12/2014	First draft send to QA
1.1	20/12/2014	Final version

## Contents

<b>1</b>	<b>Introduction</b>	<b>4</b>
1.1	Transport of hydrogen in the bulk of materials . . . . .	4
1.1.1	Diffusible hydrogen . . . . .	4
1.1.2	Trapping . . . . .	6
1.1.3	Local Equilibrium . . . . .	7
<b>2</b>	<b>FEM formulation for mass diffusion</b>	<b>8</b>
2.1	Assumptions . . . . .	8
2.2	Total form . . . . .	8
2.3	Weak form . . . . .	8
2.4	Incremental form . . . . .	9
2.5	Discrete form . . . . .	9
<b>3</b>	<b>Implementation in UMATHT and UMAT</b>	<b>11</b>
3.1	Comparison with Krom et al. . . . .	12
3.2	Derivation of stress gradients and equivalent plastic strain . . . . .	12
<b>4</b>	<b>Units and orders of magnitude</b>	<b>13</b>
4.1	Concentration conversion factors . . . . .	13
<b>5</b>	<b>Usage of the user subroutine UMATHT</b>	<b>15</b>
5.1	Geometry and element connectivity . . . . .	15
5.2	Input constants . . . . .	15

## 1 Introduction

This report summarizes the work done during the first year (2014) of ROP project toward building a modelling framework for describing mass diffusion in the bulk of materials. This framework has, within this project, the particular scope of simulating the transport stage of atomic hydrogen in iron or, more specifically, toward the site where degradation, and therefore Hydrogen Embrittlement (HE) occurs.

This introductory section is therefore devoted to this topic, with focus on the definitions of the the different material/mechanical contributions to the determination of hydrogen distribution in bulk iron.

Nevertheless, despite the clear application, the model framework is of general validity, i.e. it can be applied and used to describe mass diffusion for any solvent/solute system, given the correct parameter/inputs.

### 1.1 Transport of hydrogen in the bulk of materials

Once hydrogen is absorbed into the metal, its distribution is traditionally divided in two main contributions. The first contribution is the hydrogen at the Normal Interstitial Lattice Sites (NILS), and indicated with  $C_L$ ; the second contribution is given by hydrogen atoms trapped at the material's "imperfection" such as dislocations, grain boundaries, vacancies, inclusions or precipitates. Such contribution is indicated with  $C_T$ . These two contributions are locally in equilibrium [12], and the total final hydrogen distribution is obtained by their sum.

#### 1.1.1 Diffusible hydrogen

In the particular case of steel, iron lattice basic structure exists in two forms: body-centered cubic (bcc) ferrite (Fe- $\alpha$ ) and face-centered cubic (fcc) austenite (Fe- $\gamma$ ). The property of the steels, in terms of solubility and diffusivity, are therefore inferred from the geometrical disposition of the atoms within the lattice structures and the consequent size of the different interstitial sites. The main "engine" for hydrogen mobility is given by the concentration gradients which is generated, for instance, due to hydrogen adsorption from external sources. Fick's first law relates the diffusive flux to the concentration field, by postulating that the flux goes from regions of high concentration to regions of low concentration, with a magnitude that is proportional to the concentration gradient (spatial derivative) [5]. In one (spatial) dimension:

$$\text{Fick's first law: } J = -D \left( \frac{\partial C_L}{\partial x} \right) \quad (1)$$

where  $J$  is the hydrogen flux,  $C_L$  is the diffusible hydrogen,  $D$  is the diffusion coefficient or diffusivity, which is proportional to the velocity of the diffusing particle, and  $x$  is the position. The negative sign arises because diffusion occurs in the direction opposite to the direction of increasing concentration. It has to be noted that Fick's first law, as written in Eq. 1, is consistent only for isotropic medium whose structure and diffusion properties are the same relatively to all directions. Fick's first law applies to steady state systems, where concentration keeps constant. In many cases of diffusion, the concentration within the diffusion volume however changes with time. With some calculations based on the first Fick's law and mass balance, Fick's second law in the case of 3-dimensional diffusion is obtained:

$$\text{Fick's second law: } \frac{\partial C_L}{\partial t} = -D \nabla^2 C_L \quad (2)$$

where  $t$  is time and  $\nabla$  is the *del* operator. In a 3D system with perpendicular coordinates ( $x, y, z$ ), this is a Cartesian coordinate system  $R^3$ , *del* is defined as:

$$\nabla = i \frac{\partial}{\partial x} + j \frac{\partial}{\partial y} + k \frac{\partial}{\partial z} \quad (3)$$

where  $i, j$  and  $k$  are the unit-vectors in the direction of the respective coordinate (the standard basis in  $R^3$ ).

Eq. 1 and 2 defines just the basic laws to describe hydrogen flux within an unstressed perfect lattice structure. In reality, the correct way to look at hydrogen diffusion through the steel is not as a straight line trajectory. As showed by Jiang and Carter [7] through first principle Density Functional Theory (DFT) calculations, H-atom diffuses through bcc Fe not via a straight trajectory line, but rather jumps from one t-site (t stays for tetrahedral) to another neighboring t-site by a curve path distorted toward octahedral sites.

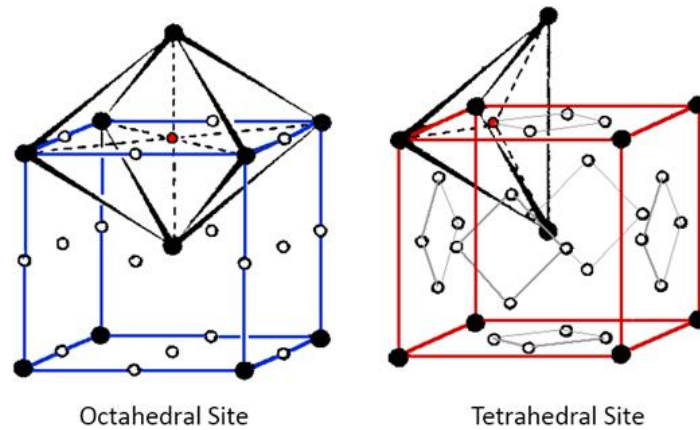


Figure 1: Interstitial sites present in a BCC crystal structure [2].

As mentioned before, the small size of hydrogen allows higher solubility and greater mobility than other elements. However, hydrogen atoms are still larger than the interstitial sites:  $r_H = 0.53 \text{ \AA}$ , to be compared with  $r_i = 0.19 \text{ \AA}$  for o-sites in austenitic steel (the largest among the interstitial sites in steels). This induces a distortion of the host lattice and the resulting stress and displacement fields interact with other defects. The “strength” of this type of interaction is quantified by the hydrogen’s partial molar volume, i.e. the unconstrained volume dilatation of the metal containing one mole of hydrogen. An isochore introduction of hydrogen into a lattice creates a hydrostatic compression stress [3, 4]. Thereby, the mean hydrostatic stress affects the hydrogen solubility in the host metal, and hydrostatic stress gradients affect hydrogen diffusion [10]. Therefore, a more complete description for hydrogen diffusion should consider both for hydrogen concentrations and hydrostatic stress gradients. Abaqus [1] provides the following mass diffusion equation already embedded with the finite element code:

$$\frac{\partial C_L}{\partial t} = D \nabla^2 C_L + D \left( \frac{V_H}{R(T - T^Z)} \right) \nabla C_L \nabla p + D \left( \frac{V_H}{R(T - T^Z)} \right) C_L \nabla^2 p \quad (4)$$

In conclusion, relation 4 indicates that the energy necessary to introduce a hydrogen atom in the lattice increases together with the decrease of hydrogen concentration gradients and is decreased by dilatational hydrostatic stress: areas in front of cracks are therefore zones of strong accumulation for diffusible hydrogen.

### 1.1.2 Trapping

Hydrogen distribution is determined not only by the concentration gradients and lattice dilatation due to hydrostatic stress as described by 4, but it is recognized that also trapping is a potent mechanism for H segregation [12], [16], [13]. Traps can be seen as local perturbations of the lattice structure: typical traps are dislocations, vacancies, grain boundaries, phase boundaries, inclusions and precipitates. Trapping reduces the amount of mobile hydrogen inferring a decrease of the apparent diffusivity and increasing the local solubility favoring segregation. The ability of traps to “hold” hydrogen atoms is associated with hydrogen binding energy and activation energy for hydrogen release ( $\Delta E_T$ ) and, based on the values of these terms, trapping sites are usually categorized as reversible and irreversible traps. Reversible traps concern binding energies usually lower than 60/70 *kJ/mol* [17] and hydrogen can typically be released by simple tempering. On the contrary, for irreversible traps normal tempering result uneffective since the energy barrier to be overcome in order for hydrogen to regain mobility is higher. A typical example of irreversible trap sites is the interface between non-metallic inclusion or precipitates jump.

Of special interest is hydrogen trapping related to dislocation which has been studied extensively in the last decades [16],[6],[3], [4], [14]. In a nutshell, dislocations, which in metals are associated with the plastic deformation development, can be imagined as moving traps, having therefore a great impact on the total hydrogen distribution in the material. Kumnick and Johnson [9] firstly calculated the variation of the amount and the densities of trapping sites in steel at different cold-working levels. Their results are graphically presented (see Fig. 2) by Sofronis and McMeeking [15], who also proposed the following mathematical fitting:

$$\text{Log}(N_T) = 23.26 - 2.33 \exp(-5.5\epsilon_p) \quad (5)$$

where  $N_T$  is the trap density and  $\epsilon_p$  is the equivalent plastic strain: trap densities are independent on temperature, increase sharply with deformation at low deformation levels and more gradually with further deformation, reaching saturation at plastic strain greater than 80%.

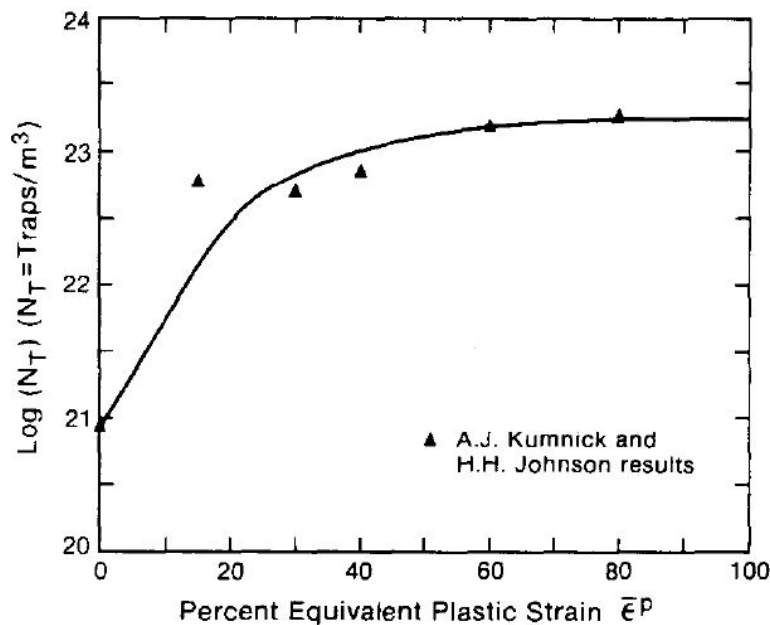


Figure 2: Relation between number of traps and plastic strain fitted from Kumnick and Johnson experimental results [15].

### 1.1.3 Local Equilibrium

As summarized in the previous sections, two types of hydrogen concentrations can be distinguished: hydrogen in NILS, indicated by  $C_L$  and hydrogen in traps,  $C_T$ . Oriani [12] proposed the principle that for rapid trap filling kinetics, these two “populations” are locally in equilibrium. Such principle is described by the relation

$$C_T = \frac{K \frac{\alpha N_T}{\beta N_L} C_L}{1 + \frac{K}{\beta N_L} C_L} \quad (6)$$

where  $N_T$  and  $N_L$  are the available sites for hydrogen in traps and in lattice sites, respectively.  $N_L$  is calculated through:

$$N_L = \frac{N_A}{V_M} \quad (7)$$

where  $N_A$  is the Avogadro number and  $V_M$  is the molar volume of iron.  $\alpha$  and  $\beta$  are parameters which indicates the site occupancies for traps and lattice sites, respectively. The parameter  $\alpha$  is taken as 1 while  $\beta$  is assigned to 6 under assumption of tetrahedral site occupancy.  $K_T$  represents the equilibrium constant between lattice and trap sites:

$$K_T = \exp\left(\frac{-\Delta E_T}{RT}\right) \quad (8)$$

$\Delta E_T$  is the trap binding energy, always negative, and assigned according to the type of traps under consideration [9]. The inherent meaning of Oriani’s equilibrium principle is that, at local level, the two populations of hydrogen affect one another: variations of lattice hydrogen modifies the reversibly trapped hydrogen and viceversa. It is important also to point out that such theory considers exclusively reversible traps.



## 2 FEM formulation for mass diffusion

The FEM formulation of hydrogen diffusion here implemented has been derived from by [8] which has been obtained through Eq. 1. to Eq. 8 . The formulation is revisited here.

### 2.1 Assumptions

The system is modeled by

$$\dot{C}_L + \dot{C}_T + \bar{\nabla} \cdot \bar{J} = 0 \quad (9)$$

with

$$\bar{J} = -D_L \bar{\nabla} C_L - D_p C_L \bar{\nabla} p \quad (10)$$

$$\frac{C_T}{N_T - C_T} = \frac{C_L}{N_L - C_L} K_T \quad (11)$$

$$K_T = e^{-\frac{\Delta E_T}{RT}} \quad (12)$$

$$D_p = \frac{D_L V_H}{RT} \quad (13)$$

### 2.2 Total form

By multiplying denominator and divisor by  $C_L$ , (11) can be rewritten as

$$C_T = \frac{K_T N_T C_L}{N_L + C_L (K_T - 1)} \quad (14)$$

Assuming  $N_L$  and  $K_T$  not to vary with time

$$\frac{\partial C_L}{\partial t} + \frac{\partial C_T}{\partial t} = \frac{\partial C_L}{\partial t} + \frac{\partial C_T}{\partial C_L} \frac{\partial C_L}{\partial t} + \frac{\partial C_T}{\partial N_T} \frac{\partial N_T}{\partial t} \quad (15)$$

$$= \left[ 1 + \frac{N_T N_L K_T}{(N_L + C_L (K_T - 1))^2} \right] \frac{\partial C_L}{\partial t} + \left[ \frac{K_T C_L}{N_L + C_L (K_T - 1)} \right] \frac{\partial N_T}{\partial t} \quad (16)$$

so finally

$$0 = f(C_L, \dot{C}_L) + \bar{\nabla} \cdot \bar{J}(C_L) \quad (17)$$

with

$$f(C_L, \dot{C}_L) = \left( 1 + \frac{N_T N_L K_T}{(N_L + C_L (K_T - 1))^2} \right) \dot{C}_L + \frac{K_T C_L \dot{N}_T}{N_L + C_L (K_T - 1)} \quad (18)$$

This is a single scalar non-linear differential equation in  $C_L$ ,  $N_T$  and  $p$ .  $C_T$  has been eliminated using (14). In the following we will assume  $N_T$  and  $p$  to be known (weak connection to another solution). We further assume all other coefficients to be known and constant in time and space.

### 2.3 Weak form

The weak form of the differential equation is obtained by requiring that for any “virtual variation”  $\delta C_L$  of the unknown field  $C_L$ , equation (17) multiplied by  $\delta C_L$  and integrated over  $\mathcal{V}$ , must be verified

$$0 = \int_{\mathcal{V}} \delta C_L f d\mathcal{V} + \int_{\mathcal{V}} \delta C_L \bar{\nabla} \cdot \bar{J} d\mathcal{V} \quad (19)$$

$$= \int_{\mathcal{V}} \delta C_L f d\mathcal{V} + \int_{\mathcal{V}} \bar{\nabla} \cdot (\delta C_L \bar{J}) d\mathcal{V} - \int_{\mathcal{V}} \bar{\nabla} \delta C_L \cdot \bar{J} d\mathcal{V} \quad (20)$$

$$= \int_{\mathcal{V}} \delta C_L f d\mathcal{V} + \int_{\mathcal{S}} \bar{n} \cdot (\delta C_L \bar{J}) d\mathcal{S} - \int_{\mathcal{V}} \bar{\nabla} \delta C_L \cdot \bar{J} d\mathcal{V} \quad (21)$$

$$0 = \int_{\mathcal{V}} \delta C_L f d\mathcal{V} + \int_{\mathcal{S}} \delta C_L \phi d\mathcal{S} - \int_{\mathcal{V}} \bar{\nabla} \delta C_L \cdot \bar{J} d\mathcal{V} \quad (22)$$

with

$$\phi = \bar{n} \cdot \bar{J} \quad (23)$$

where  $\bar{n}$  is the outward pointing normal to  $\mathcal{S}$  and  $\phi$  is the hydrogen flow out through  $\mathcal{S}$ .

The integration by parts has allowed to introduce boundary conditions: at any point of  $\mathcal{S}$ , either  $\phi$  must be known (non-essential boundary condition) or  $\delta C_L$  must be zero (essential boundary condition).

## 2.4 Incremental form

The incremental form of  $E = 0$  in  $C_L$  and  $\dot{C}_L$  is

$$0 = E + \frac{\partial E}{\partial C_L} \Delta C_L + \frac{\partial E}{\partial \dot{C}_L} \Delta \dot{C}_L \quad (24)$$

and hence the incremental form of (22) is (assuming  $\phi$  to be a known boundary condition)

$$0 = \int_{\mathcal{V}} \delta C_L f \, d\mathcal{V} + \int_{\mathcal{S}} \delta C_L \phi \, d\mathcal{S} - \int_{\mathcal{V}} \bar{\nabla} \delta C_L \cdot \bar{J} \, d\mathcal{V} \quad (25)$$

$$+ \int_{\mathcal{V}} \delta C_L \frac{\partial f}{\partial C_L} \Delta C_L \, d\mathcal{V} - \int_{\mathcal{V}} \bar{\nabla} \delta C_L \cdot \frac{\partial \bar{J}}{\partial C_L} \Delta C_L \, d\mathcal{V} \quad (26)$$

$$+ \int_{\mathcal{V}} \delta C_L \frac{\partial f}{\partial \dot{C}_L} \Delta \dot{C}_L \, d\mathcal{V} \quad (27)$$

or

$$\begin{aligned} 0 = & \int_{\mathcal{V}} \delta C_L \left[ \left( 1 + \frac{N_T N_L K_T}{(N_L + C_L (K_T - 1))^2} \right) \dot{C}_L + \frac{K_T C_L \dot{N}_T}{N_L + C_L (K_T - 1)} \right] d\mathcal{V} \\ & + \int_{\mathcal{S}} \delta C_L \phi \, d\mathcal{S} \\ & - \int_{\mathcal{V}} \bar{\nabla} \delta C_L \cdot [-D_L \bar{\nabla} C_L - D_p C_L \bar{\nabla} p] \, d\mathcal{V} \\ & + \int_{\mathcal{V}} \delta C_L \left[ \frac{-2(K_T - 1) N_T N_L K_T \dot{C}_L}{(N_L + C_L (K_T - 1))^3} + \frac{K_T N_L \dot{N}_T}{(N_L + C_L (K_T - 1))^2} \right] \Delta C_L \, d\mathcal{V} \\ & - \int_{\mathcal{V}} \bar{\nabla} \delta C_L \cdot [-D_L \bar{\nabla} - D_p \bar{\nabla} p] \Delta C_L \, d\mathcal{V} \\ & + \int_{\mathcal{V}} \delta C_L \left[ 1 + \frac{N_T N_L K_T}{(N_L + C_L (K_T - 1))^2} \right] \Delta \dot{C}_L \, d\mathcal{V} \end{aligned} \quad (28)$$

## 2.5 Discrete form

Shape functions are introduced for the unknown field:

$$\Delta C_L = \bar{S}_C \cdot \Delta \bar{C}_L \quad (29)$$

$$\Delta \dot{C}_L = \bar{S}_C \cdot \Delta \dot{\bar{C}}_L \quad (30)$$

$$\delta C_L = \bar{S}_C \cdot \delta \bar{C}_L \quad (31)$$

The gradients of these shape functions will be used:

$$\bar{\bar{G}}_C = \bar{\nabla} \bar{S}_C \quad (32)$$

Since (28) must hold for any  $\delta C_L$ , it must hold for any  $\delta \bar{C}_L$  and we obtain:

$$\begin{aligned}
\bar{0} &= \int_{\mathcal{V}} \bar{S}_C \left[ \left( 1 + \frac{N_T N_L K_T}{(N_L + C_L (K_T - 1))^2} \right) \dot{C}_L + \frac{K_T C_L \dot{N}_T}{N_L + C_L (K_T - 1)} \right] d\mathcal{V} \\
&+ \int_S \bar{S}_C \phi d\mathcal{S} \\
&- \int_{\mathcal{V}} \bar{\bar{G}}_C^T \cdot [-D_L \bar{\nabla} C_L - D_p C_L \bar{\nabla} p] d\mathcal{V} \\
&+ \int_{\mathcal{V}} \bar{S}_C \left[ \frac{-2(K_T - 1) N_T N_L K_T \dot{C}_L}{(N_L + C_L (K_T - 1))^3} + \frac{K_T N_L \dot{N}_T}{(N_L + C_L (K_T - 1))^2} \right] \bar{S}_C d\mathcal{V} \cdot \Delta \bar{C}_L \\
&- \int_{\mathcal{V}} \bar{\bar{G}}_C^T \cdot [-D_L] \bar{\bar{G}}_C d\mathcal{V} \cdot \Delta \bar{C}_L \\
&- \int_{\mathcal{V}} \bar{\bar{G}}_C^T \cdot [-D_p \bar{\nabla} p] \bar{S}_C d\mathcal{V} \cdot \Delta \bar{C}_L \\
&+ \int_{\mathcal{V}} \bar{S}_C \left[ 1 + \frac{N_T N_L K_T}{(N_L + C_L (K_T - 1))^2} \right] \bar{S}_C d\mathcal{V} \cdot \Delta \dot{\bar{C}}_L
\end{aligned} \tag{33}$$

This can be rewritten

$$\bar{\bar{K}} \cdot \Delta \bar{C}_L + \bar{\bar{M}} \cdot \Delta \dot{\bar{C}}_L = \bar{F} \tag{34}$$

with

$$\begin{aligned}
\bar{\bar{K}} &= \int_{\mathcal{V}} \bar{S}_C \left[ \frac{-2(K_T - 1) N_T N_L K_T \dot{C}_L}{(N_L + C_L (K_T - 1))^3} + \frac{K_T N_L \dot{N}_T}{(N_L + C_L (K_T - 1))^2} \right] \bar{S}_C d\mathcal{V} \\
&+ \int_{\mathcal{V}} \bar{\bar{G}}_C^T \cdot [D_L] \bar{\bar{G}}_C d\mathcal{V} \\
&+ \int_{\mathcal{V}} \bar{\bar{G}}_C^T \cdot [D_p \bar{\nabla} p] \bar{S}_C d\mathcal{V}
\end{aligned} \tag{35}$$

$$\bar{\bar{M}} = \int_{\mathcal{V}} \bar{S}_C \left[ 1 + \frac{N_T N_L K_T}{(N_L + C_L (K_T - 1))^2} \right] \bar{S}_C d\mathcal{V} \tag{36}$$

$$\begin{aligned}
\bar{F} &= - \int_{\mathcal{V}} \bar{S}_C \left[ \left( 1 + \frac{N_T N_L K_T}{(N_L + C_L (K_T - 1))^2} \right) \dot{C}_L + \frac{K_T C_L \dot{N}_T}{N_L + C_L (K_T - 1)} \right] d\mathcal{V} \\
&- \int_S \bar{S}_C \phi d\mathcal{S} \\
&- \int_{\mathcal{V}} \bar{\bar{G}}_C^T \cdot [D_L \bar{\nabla} C_L + D_p C_L \bar{\nabla} p] d\mathcal{V}
\end{aligned} \tag{37}$$

Note that (37) does not contain second order derivatives if either  $C_L$  or  $p$ , thanks to the sequence weak form-partial integration-incremental form. The alternative sequence incremental form-weak form-partial integration yields the same formulation, except for second derivatives in  $\bar{F}$ .

For the special case in which there are no traps (hydrogen is only dissolved in the lattice), it is found by setting  $N_T = \dot{N}_T = 0$ , or equivalently,  $K_T = 0$  in the above expressions.

### 3 Implementation in UMATHT and UMAT

As mentioned in the previous sections, Abaqus' option for mass transfer analysis cannot be used because it does not allow to specify the non-linear diffusivity and solubility due to dislocation traps. However, an alternative way can be found by taking advantage of the similarity between Fourier's and Fick's law (i.e. solute concentration can be treated as temperature): the above formulation is implemented in Abaqus by using UMATHT, a user definable subroutine for heat transfer.

The following table shows the relation between the inputs and outputs to MATHT and the present formulation.

Function	Variable	Heat Transfer	Mass Diffusion
UMATHT	U	$U(\theta, t)$	$C_L + C_T$
	DUDT	$\frac{\partial U}{\partial \theta}$	$\frac{\partial(C_L+C_T)}{\partial C_L} = 1 + \frac{N_T N_L K_T}{(N_L + C_L(K_T - 1))^2}$
	DUDG	$\frac{\partial U}{\partial \bar{\nabla} \theta}$	$\frac{\partial(C_L+C_T)}{\partial \bar{\nabla} C_L} = \bar{0}$
	TEMP	$\theta$	$C_L$
	DTEMP	$\Delta \theta$	$\Delta C_L$
	DTEM DX	$\bar{\nabla} \theta$	$\bar{\nabla} C_L$
	FLUX	$\bar{f}(\theta, \bar{\nabla} \theta)$	$\bar{J}(C_L, \bar{\nabla} C_L) = -D_L \bar{\nabla} C_L - D_p C_L \bar{\nabla} p$
	DFDT	$\frac{\partial \bar{f}}{\partial \theta}$	$\frac{\partial \bar{J}}{\partial C_L} = -D_p \bar{\nabla} p$
	DFDG	$\frac{\partial \bar{f}}{\partial \bar{\nabla} \theta}$	$\frac{\partial \bar{J}}{\partial \bar{\nabla} C_L} = -D_L$
UMAT	RPL	$\Delta U$	0
	DDSDDT	$\frac{\partial \Delta \bar{\sigma}}{\partial \theta}$	$\frac{\partial \Delta \bar{\sigma}}{\partial C_L}$
	DRPLDE	$\frac{\partial \Delta U}{\partial \bar{\epsilon}}$	$\frac{K_T C_L}{N_L + C_L(K_T - 1)} \frac{\partial N_T}{\partial \bar{\epsilon}}$
	DRPLDT	$\frac{\partial \Delta U}{\partial \theta}$	$\frac{-2(K_T - 1)N_T N_L K_T}{(N_L + C_L(K_T - 1))^3}$

Table 1: Correspondence with UMATHT and UMAT

Considering the expressions in Table 1, it is conspicuous that some of the terms found in Section 2.5 are absent:

$$\frac{-2(K_T - 1)N_T N_L K_T \dot{C}_L}{(N_L + C_L(K_T - 1))^3} + \frac{K_T N_L \dot{N}_T}{(N_L + C_L(K_T - 1))^2}$$

does not appear, so Abaqus can not compute  $\bar{K}$  accurately, which will affect the convergence rate. Following [11], we can use the fact that U at the end of a step is to be provided by UMATHT to introduce the term

$$\frac{K_T C_L \dot{N}_T}{N_L + C_L(K_T - 1)}$$

Thinking of a future extension to coupled analysis (diffusion and continuum mechanics), the absence of a matrix containing the term

$$\frac{K_T C_L}{N_L + C_L (K_T - 1)}$$

implies a weak connection between the analyses, which may be a source of convergence problem.

Following [11], UMATHHT allows an exact and (thought not Newton-optimal) solution of the uncoupled hydrogen diffusion problem. Moriconi [11] further uses this UMATHHT implementation in a coupled diffusion-mechanical analysis. Apparently, Abaqus limits what mechanical material models can be used in a coupled analysis, so it was necessary to implement UMAT to provide the relevant material plasticity model. So the coupled analysis was implemented without implementing UEL (User defined ELEMENT subroutine). Note that this does not allow to model a strongly coupled problem (due to the above-mentioned missing term), for that it seems necessary to implement a complete element (UEL).

### 3.1 Comparison with Krom et al.

For large  $K_T$ , one can introduce the approximation  $K_T - 1 \approx K_T$ . Then it is possible to show that

$$\frac{\partial C_T}{\partial C_L} = \frac{C_T \left(1 - \frac{C_T}{N_T}\right)}{C_L} \quad (38)$$

$$\frac{\partial C_T}{\partial N_T} = \frac{C_T}{N_T} \quad (39)$$

so that the differential equation they solve is the correct one (even though they offer no proof for it in that publication).

### 3.2 Derivation of stress gradients and equivalent plastic strain

In our solution, the gradient of the pressure in one element is computed as follow:

The pressure at the Gauss points (center) of all neighboring elements is considered and a linear interpolation of the pressure as a function of position in the deformed mesh is introduced. The slope of this linear relation is used as a pressure gradient. This is just one of many possible approaches to finding the pressure gradient. All of them have in common that they are imperfect (computing slopes on numerical data is only apparently easy). Nevertheless, it is not known which approach Abaqus is used to compute the gradient.

The pressure is given by Abaqus as the third stress invariant for the integration point. The stress invariants can be read by calling `GETVRM()` and specify 'SINV' as the value for the parameter VAR.

The plastic strain is given by Abaqus as the seventh plastic strain value for the integration point. The strain values can be read by calling `GETVRM()` and specify 'PE' as the value for the parameter VAR.

## 4 Units and orders of magnitude

In order to build a model of the most general validity, particular attention needs to be put into the use of the unit system as well as in the list of the constants. The modelling framework is therefore built buy using constants which will eventually allow the study of mass diffusion of systems which are different than hydrogen/iron.

The unit system used is MPa meaning that the basic units are : mass in [tonne], length in [mm], time in [s], temperature in [K], pressure in [MPa], energy in [mJ] and so forth. Table 2 summarises the units for the quantities described in the previous section along with their expected order of magnitude for hydrogen/iron system.

Symbol	Order of magnitude	Unit
$C_L$		$mol \cdot mm^{-3}$
$C_T$		$mol \cdot mm^{-3}$
$N_L$	$\approx 10^{-04}$	$mol \cdot mm^{-3}$
$N_T$	$0.16603 \cdot 10^{N_{T1} - N_{T2}} \cdot e^{N_{T3} \cdot \epsilon_P}$ *	$mol \cdot mm^{-3}$
$N_{T1}$	$-8.74$ *	$mol \cdot mm^{-3}$
$N_{T2}$	$2.33$ *	
$N_{T3}$	$-5.5$ *	
$\bar{J}$		$mol \cdot m^{-2} \cdot s^{-1}$
$\Delta E_T$	$\approx 10^6$	$mol^{-1} \cdot tonne \cdot mm^2 \cdot s^{-2}$
$R$	$8.314 \cdot 10^3$	$mol^{-1} \cdot K^{-1} \cdot tonne \cdot mm^2 \cdot s^{-2}$
$T$	$293.$	$K$
$\bar{\nabla} C_L$		$mol \cdot mm^{-4}$
$D_L$	$\approx 10^{-6}$	$mm^2 \cdot s^{-1}$
$D_p$	$\approx 10^{-9}$	$tonne^{-1} \cdot mm^3 \cdot s$
$p$		$tonne \cdot mm^{-1} \cdot s^{-2} (MPa)$
$\bar{\nabla} p$		$tonne \cdot mm^{-2} \cdot s^{-2}$

Table 2: Units and orders of magnitude (\*: constants obtained form Sofronis and McMeeking [15] interpolation of Kumnick and Johnson[9] experimental data)

### 4.1 Concentration conversion factors

An important issue is related to different unit systems used for defining concentrations in literature. The most common are: weight part per million ( $wppm$ ), atomic part per million ( $appm$ ), and number of hydrogen atoms per cubic meter of iron ( $at_H \cdot m_{Fe}^{-3}$ ). In the model developed here concetration values are defined as mole of solute per millimeter cube of solvent, which allows for caculations which are totally independent on the particular solute/solvent systems under study. The need for a sistematic table for conversion between all different systems arises. The conversion formulas are therefore:

$$C [mol \cdot mm^{-3}] = C [wppm] \cdot \rho_{Fe} [tonne \cdot mm^{-3}] \cdot (z_H [tonne \cdot mol^{-1}])^{-1} \quad (40)$$

$$C [appm] = C [wppm] \cdot z_{Fe} [tonne \cdot mm^{-3}] \cdot (z_H [tonne \cdot mol^{-1}])^{-1} \quad (41)$$

$$C [at_H \cdot m_{Fe}^{-3}] = C [wppm] \cdot n_A [atoms \cdot mol^{-1}] \cdot (z_H [tonne \cdot mol^{-1}] \cdot \rho_{Fe} [tonne \cdot mm^{-3}])^{-1} \quad (42)$$

$$C [mol \cdot mm^{-3}] = C [at_H \cdot m_{Fe}^{-3}] \cdot 10^{-9} [m^3 \cdot mm^{-3}] \cdot (n_A [atoms \cdot mol^{-1}])^{-1} \quad (43)$$

$$C [appm] = C [at_H \cdot m_{Fe}^{-3}] \cdot z_{Fe} [tonne \cdot mm^{-3}] \cdot (n_A [atoms \cdot mol^{-1}] \cdot \rho_{Fe} [tonne \cdot mm^{-3}])^{-1} \quad (44)$$

The constants that are necessary to perform the conversions described above (N.B. the constants defined below and the consequently calculated conversion factors are relative to hydrogen/iron system) are the following:

$V_M$  : *Molar Volume* :  $7.119 \cdot 10^{-6} m^3 \cdot mol^{-1} = 7.119 \cdot 10^3 mm^3 \cdot mol^{-1}$  which indicates the volume occupied by one mole of substance at a given temperature and pressure;

$V_H$  : *Partial Molar Volume* :  $2 \cdot 10^{-6} m^3 \cdot mol^{-1} = 2 \cdot 10^3 mm^3 \cdot mol^{-1}$  it is a thermodynamic quantity which indicates the unconstrained volume dilatation of a metal (iron in this case) due to the absorption/introduction of one mole of a solute (hydrogen);

$z_H$  : *Hydrogen Molar Mass* :  $1.008 g \cdot mol^{-1} = 1.008 \cdot 10^{-6} tonne \cdot mol^{-1}$  mass of an atom of hydrogen;

$z_{Fe}$  : *Iron Molar Mass* :  $55.845 g \cdot mol^{-1} = 55.845 \cdot 10^{-6} tonne \cdot mol^{-1}$  mass of an atom of pure iron;

$n_A$  : *Avogadro Number* :  $6.023 \cdot 10^{23} atoms \cdot mol^{-1}$  it defines the number of atoms per mole for any substance;

$\rho_{Fe}$  : *Iron Density* :  $7.8747 tonne \cdot m^{-3} = 7.8747 \cdot 10^{-9} tonne \cdot mm^{-3}$ .

Finally, Table 3 reports conversion factors as calculated by formulas in the group of Eq. (44) (unit of the value to convert “enters” from the column and the converted results “exit” from the row):

<b>CONC</b>	<i>wppm</i>	<i>appm</i>	$at_H \cdot m_{Fe}^{-3}$	$mol \cdot mm^{-3}$
<i>wppm</i>	1	55.402	$4.70 \cdot 10^{30}$	$7.81 \cdot 10^{-3}$
<i>appm</i>	0.01805	1	$8.493 \cdot 10^{28}$	$1.41 \cdot 10^{-10}$
$at_H \cdot m_{Fe}^{-3}$	$2.12 \cdot 10^{-31}$	$1.17 \cdot 10^{-29}$	1	$1.66 \cdot 10^{-33}$
$mol \cdot mm^{-3}$	128	$7.092 \cdot 10^9$	$6.023 \cdot 10^{32}$	1

Table 3: Concentration conversion factors

## 5 Usage of the user subroutine UMATHT

### 5.1 Geometry and element connectivity

UMATHT reads the geometry (node positions) and element connectivity from a file `topology.dat`. This file needs to be generated before the calculation can start. A separate program, `ReadTopology` has been created to produce the `topology.dat` file. This program requires that this information is available in a `*.fil` file.

Instruct Abaqus to produce a `.fil` file by inserting adding code like this in the input file:

```
**
** OUTPUT REQUESTS
**
*Restart, write, frequency=0
**
*Output, History
*Element Output
**
*El File, Position=Integration Point
COORD
**
** FIELD OUTPUT: F-Output-1
**
*Output, field, variable=PRESELECT
*Output, history, frequency=0
*End Step
```

To produce the `*.fil` file, run Abaqus with the command `datacheck`:

```
abaqus datacheck interactive user="UMATHT.OBJ" job="myjobname" input="myjobname.inp"
```

The file `topology.dat` can then be produced by running

```
abaqus readTopology myjobname
```

### 5.2 Input constants

To specify a material that uses the formulation in UMATHT, specify the material like this in the input file of Abaqus:

```
*User Material, constants=10, type=THERMAL
```

It should be followed by two lines containing the a list of 10 parameters; 8 on the first line and 2 on the last line:

1.  $D_L$ : Mass diffusivity
2.  $D_P$ :  $\text{Kappa} * \text{Solubility} * \text{Diffusivity}$
3.  $V_M$ : Volume of available sites for hydrogen in lattice
4. Curve parameter  $C_0$  for  $N_T = C_0 10^{(C_1 - C_2 e^{(C_3 E_P)})}$
5. Curve parameter  $C_1$  for  $N_T$
6. Curve parameter  $C_2$  for  $N_T$
7. Curve parameter  $C_3$  for  $N_T$



8.  $E_B$ : Trap binding energy
9. Material temperature in Kelvin (used to calculate  $K_T$ )
10. R: Universal gas constant (with units consistent with  $E_B$  and material temperature).

Example:

```
*USER MATERIAL, constants=10, type=THERMAL
** DL          DP          VM          NT_C0          NT_C1          NT_C2          NT_C3          EB
3.99E-6,      3.4629E-9,    7.116E+3,    0.16603,     -8.740,       2.330,       -5.5,       -28.8E+6
** T          R
293.15,      8.3144621E+3
```

\*\* in front of the line means that the line is commented while \*indicates an Abaqus command line with appropriate keywords.

## References

- [1] ABAQUS. Version 6.11. analysis user's manual. *ABAQUS Inc.*, 2012.
- [2] W.D. Callister and D.G. Rethwisch. *Materials science and engineering: an introduction*. John Wiley and Sons New York, 1997.
- [3] J.P. Chateau, D. Delafosse, and T. Magnin. Numerical simulations of hydrogen-dislocation interactions in fcc stainless steels.: part i: hydrogen-dislocation interactions in bulk crystals. *Acta materialia*, 50(6):1507–1522, 2002.
- [4] J.P. Chateau, D. Delafosse, and T. Magnin. Numerical simulations of hydrogen–dislocation interactions in fcc stainless steels.: part ii: hydrogen effects on crack tip plasticity at a stress corrosion crack. *Acta materialia*, 50(6):1523–1538, 2002.
- [5] J. Crank. *The mathematics of diffusion*. Oxford University Press, USA, 1979.
- [6] D. Delafosse and T. Magnin. Hydrogen induced plasticity in stress corrosion cracking of engineering systems. *Engineering Fracture Mechanics*, 68(6):693–729, 2001.
- [7] D.E. Jiang and E.A. Carter. Diffusion of interstitial hydrogen into and through bcc fe from first principles. *Physical Review B*, 70(6):64102, 2004.
- [8] A.H.M. Krom, R.W.J. Koers, and A. Bakker. Hydrogen transport near a blunting crack tip. *Journal of the Mechanics and Physics of Solids*, 47(4):971–992, 1999.
- [9] A.J. Kunnick and H.H. Johnson. Deep trapping states for hydrogen in deformed iron. *Acta Metallurgica*, 28(1):33–39, 1980.
- [10] J.C.M. Li, R.A. Oriani, and L.S. Darken. The thermodynamics of stressed solids. *Zeitschrift fur Physikalische Chemie*, 49(3-5):271–290, 1966.
- [11] C. Moriconi. Modelisation de la propagation de fissure de fatigue assistee par l'hydrogene gazeux dans le materiaux metalliques. *These de doctorat, Ecole Nationale Supérieure de Mecanique et d'Aerotechnique*, 2012.
- [12] R.A. Oriani. The diffusion and trapping of hydrogen in steel. *Acta Metallurgica*, 18(1):147–157, 1970.
- [13] G.M. Pressouyre. Trap theory of hydrogen embrittlement. *Acta Metallurgica*, 28(7):895–911, 1980.
- [14] I.M. Robertson. The effect of hydrogen on dislocation dynamics. *Engineering Fracture Mechanics*, 68(6):671–692, 2001.
- [15] P. Sofronis and R.M. McMeeking. Numerical analysis of hydrogen transport near a blunting crack tip. *Journal of the Mechanics and Physics of Solids*, 37(3):317–350, 1989.
- [16] A. West and M. Louthan. Dislocation transport and hydrogen embrittlement. *Metallurgical and Materials Transactions A*, 10(11):1675–1682, 1979.
- [17] T. Zakroczymski. Adaptation of the electrochemical permeation technique for studying entry, transport and trapping of hydrogen in metals. *Electrochimica Acta*, 51(11):2261–2266, 2006.



Technology for a better society  
[www.sintef.no](http://www.sintef.no)